Articles

Preparation and Characterization of Cross-Linked Composite Polymer Electrolytes

Jun Hou and Gregory L. Baker*

Department of Chemistry and Center for Fundamental Materials Research, Michigan State University, East Lansing, Michigan 48824

Received July 10, 1997. Revised Manuscript Received August 3, 1998

Cross-linkable composite electrolytes were prepared from poly(ethylene glycol) dimethyl ether (PEGDME)-500, $LiClO_4$, fumed silica, and 10 wt % methyl, butyl, or octyl methacrylate. The silicas used were chemically modified by attaching methacrylate groups to the silica surface through C_8 and C_3 tethers. Before cross-linking, the electrolytes were thixotropic and had ionic conductivities of $>2 \times 10^{-4}$ S/cm. After ultraviolet (UV)-induced cross-linking, the electrolytes were rubbery and dimensionally stable, and the conductivities were unchanged. Conductivity, extraction, and thermal analysis data all support a model where the added methacrylate monomer and growing polymer chains phase separate from the electrolyte phase during photopolymerization to yield a methacrylate-rich silica/polymer phase and little or no polymer in the PEGDME-500 phase. Thus, the mechanical properties of the composite electrolyte and its ionic conductivity are decoupled and can be optimized independently.

A long-standing goal of polymer electrolyte research is the preparation of an electrolyte that combines the processing characteristics of conventional thermoplastics with the ionic conductivity of low molar mass liquids. Despite extensive research efforts, the conductivities of the best solid polymer electrolytes range from 1 to 5×10^{-5} S/cm, which is too low for important applications such as electrolytes for lithium ion batteries.[1] The principal reason for the low ionic conductivity is that the conduction mechanism for ions in polymers is similar to that of liquids; that is, there is tight binding of the cation to the lone pairs of electrons of the ether linkages in the polymer matrix. Thus the mobility of ions in polymers is closely correlated to the flexibility of the polymer chains. Successful strategies for obtaining materials with higher conductivities include decreasing the polymer glass transition temperature (T_g),[2−5] (and thus increasing the flexibility of the polymer backbone), minimizing polymer matrix crystallinity,[6−8] or using branched polymers.[9−12] In the best systems, the conductivities of lithium salt/polymer complexes that have good mechanical properties reach $2-5 \times 10^{-5}$ S/cm. Given the broad range of polymer structures that have been investigated as potential electrolytes, it is unlikely that new polymers will be prepared that have significantly higher conductivities.

Research on solid polymer electrolytes has largely been supplanted by studies of gel electrolyte systems.[13,14] Gel electrolytes, typically polymers swollen with low molecular weight liquid electrolytes, can have room-temperature conductivities as high as 10^{-3} S/cm, which is comparable to liquid electrolytes.[15−18] Con-

(1) For overviews of polymer electrolyte research, see (a) MacCallum, J. R.; Vincent, C. A. *Polymer Electrolyte Reviews-1*; Elsevier Applied Science: New York, 1987; Vol. 1. (b) MacCallum, J. R.; Vincent, C. A. *Polymer Electrolyte Reviews-2*; Elsevier Applied Science: New York, 1989; Vol. 2. (c) Gray, F. M. *Solid Polymer Electrolytes: Fundamentals and Applications*; VCH: New York, 1991. (d) Bruce, P. G.; Vincent, C. A. *J. Chem. Soc., Faraday Trans. 1* **1993**, *89*, 3187.

(2) Blonsky, P. M.; Shriver, D. F.; Austin, P.; Allcock, H. R. *J. Am. Chem. Soc.* **1984**, *106*, 6854.

(3) Fish, D.; Khan, I. M.; Wu, E.; Smid, J. *Br. Polym. J.* **1988**, *20*, 281.

(4) Allcock, H. R.; Napierala, M. E.; Cameron, C. G.; O'Connor, S. J. M. *Macromolecules* **1996**, *29*, 1951.

(5) Allcock, H. R.; Kuharcik, S. E.; Reed, C. S.; Napierela, M. E. *Macromolecules* **1996**, *29*, 3384.

(6) Nicholas, C. V.; Wilson, D. J.; Booth, C.; Giles, J. R. M. *Br. Polym. J.* **1988**, *20*, 289.

(7) Wieczorek, W.; Such, K.; Wycislik, H.; Plocharski, J. *Solid State Ionics* **1989**, *36*, 255.

(8) Croce, F.; Scrosati, B.; Mariotto, G. *Chem. Mater.* **1992**, *4*, 1134−1136.

(9) Xia, D. W.; Soltz, D. *Solid State Ionics* **1984**, *14*, 221.

(10) Cowie, J. M. G.; Martin, A. C. S. *Polymer* **1987**, *28*, 627.

(11) Yamaguchi, Y.; Aoki, S.; Watanabe, M.; Sanui, K.; Ogata, N. *Solid State Ionics* **1990**, *40/41*, 628.

(12) Hawker, C. J.; Chu, F.; Pomery, P. J.; Hill, D. J. T. *Macromolecules* **1996**, *29*, 3831.

(13) Kelly, I.; Owen, J. R.; Steele, B. C. H. *J. Electroanal. Chem.* **1984**, *168*, 467.

(14) Ballard, D. G. H.; Cheshire, P.; Man, T. S.; Przeworski, J. E. *Macromolecules* **1990**, *23*, 1256.

(15) Abraham, K. M.; Alamgir, M. *J. Electrochem. Soc.* **1990**, *137*, 1657.

(16) Matsumoto, M.; Ichinio, T.; Rutt, J. S.; Nishi, S. *J. Electrochem. Soc.* **1994**, *141*, 1989.

(17) Zygadlo-Monikowska, E.; Florjanczyk, Z.; Wieczorek, W. *J. M. S.-Pure Appl. Chem.* **1994**, *A31*, 1121−1134.

(18) Peramunage, D.; Pasquariello, D. M.; Abraham, K. M. *J. Electrochem. Soc.* **1995**, *142*, 1789.

10.1021/cm9704894 CCC: $15.00
Published on Web 10/20/1998

ceptually, a gel electrolyte functions as a sponge, with the polymer matrix providing mechanical stability, whereas good ionic conductivity results from the absorbed electrolyte. The polymer matrix itself is not involved in ion transport. In short, gel electrolytes have high ionic conductivities because the ionic mobility is decoupled from the polymer matrix.

Recently, inorganic fillers have been used to improve the electrochemical and mechanical characteristics of electrolytes.[7,8,19−27] For example, we recently reported that an electrolyte system prepared from surface-modified fumed silica, $LiClO_4$, and either low molecular weight poly(ethylene glycol)s (PEGs) or poly(ethylene glycol) dimethyl ethers (PEGDMEs) that have room-temperature conductivities $>10^{-4}$ S/cm.[25] More recent data show that the use of Li-imide salts instead of $LiClO_4$ gives conductivities that exceed 10^{-3} S/cm.[28] In these composite electrolyte systems, the conductivity and mechanical properties are highly decoupled. The fumed silica, which is not involved in ion transport, provides good mechanical properties, whereas the oligomeric polyethers used in the electrolyte ensure a high conductivity. In addition to having high conductivities, the composites are thixotropic, giving them important processing advantages compared with common electrolytes. Fumed silica added to low molecular weight oils and fluids can convert these low viscosity materials to gels with yield points. The gel behavior results from a chainlike structure of silica particles that link to form a three-dimensional network. When sheared, the structure is disrupted and the gel reverts to a low viscosity fluid, but with time, the fumed silica network structure is re-formed and the gel-like characteristics of the composite are restored.[29] Similarly, composite electrolytes prepared from fumed silicas can be processed as low viscosity fluids and after network formation, exhibit the mechanical characteristics of gel electrolytes.

An important extension of fumed silica-based electrolyte systems would be the ability to *permanently* lock the silica network structure to form dimensionally stable electrolytes. As shown in Scheme 1, fumed silicas functionalized with polymerizable groups could be cross-linked in a final processing step, with the cross-linking induced, in principle, by a broad range of chemical or photochemical processes. The starting point for designing such a system is the assumption that the aggregation patterns of fumed silica mixed with PEG depend on the relative magnitudes of the silica−silica (surface) and the silica−polyether interactions. In nonpolar solvents, polar fumed silicas aggregate to form strong networks that exhibit yield points. The use of more polar solvents such as alcohols or water leads to weaker structures or no gel formation. Modification of the silica surface changes the aggregation pattern. For example, R805, a commercial hydrophobic silica with surface-bound *n*-octyl groups, forms weak networks in polar solvents and stronger networks in hydrophilic solvents such as low molecular weight polyethers. Silicas whose surface groups mimic those of the solvent simply disperse to form a low viscosity liquid. In this paper, we report the preparation and characterization of a cross-linkable electrolyte system based on these principles.

Scheme 1. Preparation of Cross-Linked Fumed Silica Composites

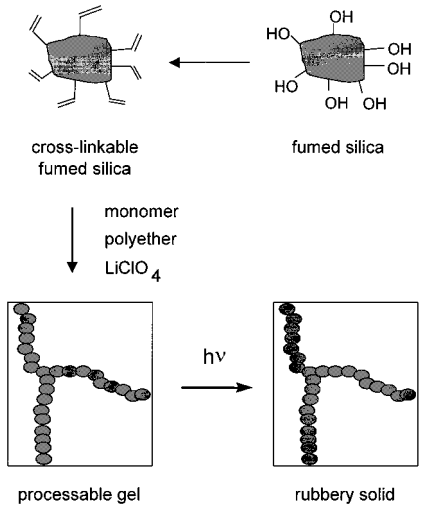

Experimental Section

Unless otherwise specified, ACS reagent grade starting materials and solvents were used as received from commercial suppliers without further purification. Aerosil A-200 was a gift from Degussa A. G., Frankfurt, Germany. This silica has a surface silanol group content of 1 mmol/g, and was stored over a half-saturated solution of NH_4NO_3 for at least 1 week prior to modification reactions. Proton and ^{13}C nuclear magnetic resonance (NMR) analyses were carried out at room temperature in deuterated chloroform ($CDCl_3$) on a Varian Gemini-300 spectrometer with the solvent proton signals as chemical shift standards. A Nicolet IR/42 spectrometer purged with dry nitrogen was used to obtain infrared (IR) spectra. Samples used were 1-cm^2 pressed pellets prepared from ≈10 mg of the various pure silicas. All spectra reported were acquired by signal averaging 32 scans at a resolution of 4 cm^{-1}. Differential scanning calorimetry (DSC) under helium and thermogravimetric analyses (TGA) in air were performed on Perkin-Elmer DSC 7 and Perkin-Elmer TGA 7 instruments, respectively, at a heating rate of 10 °C/min. For DSC measurements, the temperature was calibrated with an indium standard, and samples were initially heated to 100 °C to erase the thermal history of the sample and then were quenched to −100 °C prior to starting the run. Samples for TGA measurements were first dried in a vacuum at 120 °C overnight. Dried samples (∼5−10 mg) were held at 115 °C in the TGA apparatus until a stable weight reading was obtained, and then the run was started.

Synthesis of Acrylate-Modified Silicas. *2-(8-Chlorooctyloxy)tetrahydropyran.*[30] Over a period of 15 min, 3,4-

(19) Weston, J. E.; Steele, B. C. H. *Solid State Ionics* **1982**, *7*, 75.
(20) Plocharski, J.; Wieczorek, W. *Solid State Ionics* **1988**, *28−30*, 979.
(21) Scrosati, B. *J. Electrochem. Soc.* **1989**, *136*, 2774.
(22) Croce, F.; Bonino, F.; Panero, S.; Scrosati, B. *Philos. Mag.* **1989**, *59*, 161.
(23) Plocharski, J.; Wieczorek, W.; Przyluski, J.; Such, K. *Appl. Phys. A* **1989**, *49*, 55.
(24) Croce, F.; Passerini, S.; Selvaggi, A.; Scrosati, B. *Solid State Ionics* **1990**, *40−41*, 375.
(25) Khan, S. A.; Baker, G. L.; Colson, S. *Chem. Mater.* **1994**, *6*, 2359.
(26) Borghini, M. C.; Mastragostino, M.; Passerini, S.; Scrosati, B. *J. Electrochem. Soc.* **1995**, *142*, 2118.
(27) Appetecchi, G. B.; Dautzenberg, G.; Scrosati, B. *J. Electrochem. Soc.* **1996**, *143*, 6.
(28) Fan, J.; Fedkiw, S. *J. Electrochem. Soc.* **1997**, *144*, 399.
(29) Michael, G.; Ferch, H. *Technical Bulletin Pigments*; Degussa AG, 1993.
(30) Van, J. H.; Hershied, J. D. M. *Synthesis* **1973**, 169.

dihydro-2*H*-pyran (45 mL, 0.52 mol) was added in a dropwise manner to a magnetically stirred solution of 8-chlorooctanol (25 g, 0.15 mol) and reagent grade *p*-toluenesulfonic acid monohydrate (1.9 g, 9.8 mmol) in anhydrous 1,4-dioxane (280 mL) at room temperature. After stirring for an additional 10 min, half-saturated methanolic ammonia was added until the mixture was slightly basic. Removal of solvent gave a viscous solution that was washed with 15% aqueous sodium bicarbonate and extracted into chloroform. The organic layer was dried over $MgSO_4$ for 2 h and filtered, and the solvent was removed to yield 2-(8-chlorooctyloxy)tetrahydropyran. This material was used without further purification.

2-(7-Octenyloxy)tetrahydropyran.[31] To a 1-L round-bottomed flask were added 600 mL of dimethyl sulfoxide (DMSO) and 34 g (0.29 mol) of KO*t*-Bu. The mixture was stirred until homogeneous. The crude 2-(8-chlorooctyloxy)tetrahydropyran from the previous preparation was added through a dropping funnel over a period of 30 min. After stirring for 2 h, the mixture was extracted with pentane and was washed with half-saturated $NaHCO_3$. The organic layer was washed with distilled water and dried over $MgSO_4$. Concentration and distillation gave 27.4 g (88%) of the desired olefin as a clear oil; bp 94−96 °C/0.4 mmHg (lit.[32] bp 130 °C/12 mmHg). ^{1}H NMR ($CDCl_3$): δ 5.87−5.74 (ddt, 1H), 5.02−4.90 (m, 2H), 4.57 (t, 1H), 3.90−3.34 (m, 2H), 2.07−2.01 (m, 2H), 1.87−1.33 (m, 14H).

7-Octen-1-ol. Using a literature procedure as a guide,[30] 7.2 g (34 mmol) of 2-(7-octenyloxy)tetrahydropyran were added to 200 mL of acidified ethanol, and the mixture was heated in an oil bath to the reflux temperature for 30 min. The ethanol was removed, and the product was diluted with CH_2Cl_2 and dried over $MgSO_4$. Concentration and distillation gave 4.0 g (90% yield) of the deprotected product; bp 40 °C/0.2 mmHg) (lit[33] bp 64−66 °C/7 mmHg). ^{1}H NMR ($CDCl_3$): δ 5.88−5.74 (ddt,1H), 5.03−4.91 (m, 2H), 3.62 (t, 2H), 2.08−2.01 (dt, 2H), 1.61−1.52 (m, 2H), 1.44−1.28 (m, 6H). ^{13}C NMR ($CDCl_3$): δ 139.1, 114.2, 63.0, 33.7, 32.71, 28.9, 28.8, 25.6.

7-Octenyl Methacrylate. To a 100-mL round-bottom flask were added 30 mL of CCl_4, 4.0 g (31 mmol) of 7-octen-1-ol, and 8 g of crushed 3 Å molecular sieves. The mixture was heated to reflux, and 4.4 g (47 mmol) of methacryloyl chloride in 10 mL of CCl_4 was added over a period of 15 min under dry N_2. Heating was continued overnight. The molecular sieves were removed by filtration, and after removing the solvent, the product was purified by column chromatography (SiO_2/hexane) to yield 5.8 g (95%) of the desired methacrylate. ^{1}H NMR ($CDCl_3$): δ 6.09 (s, 1H), 5.88−5.74 (ddt,1H), 5.54 (s, 1H), 5.03−4.91 (m, 2H), 4.13 (t, 2H), 2.08−2.01 (dt, 2H), 1.94 (s, 3H), 1.71−1.60 (m, 2H), 1.44−1.30 (m, 6H). ^{13}C NMR ($CDCl_3$): δ 167.5, 138.9, 136.5, 125.1, 114.3, 64.7, 33.6, 28.7, 28.7, 28.5, 25.8, 18.3. IR: 3079, 1642 [ν(−CH═CH_2), (ν−CH_3C═CH_2)], 1713 [ν(OCO)]. MS *m*/*z*: M^+ 196.

8-(Trichlorosilyl)octyl Methacrylate. In a drybox, a 13-mm Pyrex tube was charged with 5.8 g (30 mmol) of 7-octenyl methacrylate, 0.1 mL of Speier's catalyst[34] (0.12 M H_2PtCl_6 in 2-propanol), and 4.8 g (35 mmol) of $HSiCl_3$. The tube was sealed and heated at 60 °C overnight. The volatile byproducts were removed under vacuum at room temperature and stored under vacuum until use. ^{1}H NMR ($CDCl_3$): δ 6.09 (s, 1H), 5.54 (s, 1H), 4.13 (t, 2H), 1.94 (s, 3H), 1.69−1.53 (m, 4H), 1.44−1.30 (m, 10H). ^{13}C NMR ($CDCl_3$): δ 167.5, 136.5, 125.2, 64.7, 31.7, 29.0, 28.9, 28.5, 25.9, 24.3, 22.2, 18.3. IR: 1640 [ν(−CH_3C═CH_2)], 1712 [ν(OCO)], 590, 567 [ν(Si−Cl)]. MS *m*/*z*: M^+ 331.

Preparation of Surface-Attached Methacrylates Tethered via an Octyl Side Chain. To 30 g of Aerosil 200 in a 1-L round-bottom flask were added 600 mL of toluene containing 3.0 mL (1.5 mmol) of diethylamine. The flask was attached to a mechanical shaker, and a mixture of 9.75 g (29 mmol) of 8-(trichlorosilyl)octyl methacrylate in 30 mL of toluene was added. The reaction was allowed to proceed at room temperature overnight. The product was separated by filtration and washed with three portions of both toluene and diethyl ether. The residual diethyl ether was evaporated, and the solid was transferred into a Schlenk flask and dried under vacuum at 120 °C overnight.

Preparation of Octyl-Modified Silicas with Propyl-Tethered Methacrylates. To 15 g of Aerosil 200 in a 500-mL round-bottomed flask were added 450 mL of toluene containing 1.5 mL (1.5 mmol) of diethylamine. The flask was attached to a mechanical shaker, and a mixture of 2.43 mL (9 mmol) octyltrimethoxysilane and 0.73 mL (3 mmol) trimethoxysilylpropyl methacrylate in 30 mL of toluene was added. The reaction was allowed to proceed at room temperature overnight. The product was separated by filtration and washed with three portions of toluene and three portions of diethyl ether. The residual diethyl ether was evaporated, and the solid was transferred into a Schlenk flask and dried under vacuum at 120 °C overnight.

Preparation of Composite Polymer Electrolytes. All electrolytes were prepared by the same procedure. A generic preparation is described next. To a blender cup were added 1.5 g of butyl methacrylate, 15 mg of AIBN initiator, 1.5 g of methacrylate-modified fumed silica, and 12 g of a PEGDME-500/$LiClO_4$ solution with the desired O/Li ratio. The mixture was mixed in a Waring blender for 2−5 min and then transferred to a vial. After evacuation to remove air bubbles, the sample was stored in a desiccator until used. Polymerization of the composite electrolyte was initiated with a 450 W medium-pressure Ace-Hanovia mercury lamp. Samples were placed ≈3 cm from the lamp and were exposed until rubbery. Cross-linking was performed under nitrogen and in air; curing under nitrogen allowed shorter reaction times.

Freeze-Fracture Transmission Electron Microscopy (TEM). A thin layer of the composite sample was placed on a copper plate, rapidly quenched in liquid propane, and transferred into liquid nitrogen until use. The frozen sample was fractured at −90 °C at 10^{-6} Torr. The replication was made using unidirectional shadowing with platinum and carbon at an angle of 45°. The replicas were observed in a JEOL 100 CX II transmission electron microscope.

Conductivity Measurements. The electrical properties of the samples were measured by ac impedance spectroscopy over the frequency range 6−11 MHz with an HP 4192A LF Impedance Analyzer. Samples were sandwiched between 1-cm stainless-steel disks, with the desired thickness maintained with a Teflon spacer. The disks were mechanically polished to remove burs, cleaned with alcoholic KOH, and stored in a drybox until used. The electrolyte thickness (typically 0.2−0.5 mm) was obtained by subtracting the thickness of the steel disks from the total thickness measured with a micrometer. Conductivity measurements were taken from high to low temperatures with an applied voltage of 0.1 V. Samples were held at each temperature for at least 15 min under a nitrogen gas purge before being measured. The complex impedance plots were unremarkable, with the data forming a well-defined semicircle followed by linear spike at higher impedance values. For cross-linked samples, one of the stainless-steel disks was replaced by a glass cover slip to allow optical access to the sample. The composites were polymerized as already described, and after polymerization, the glass slide was peeled off gently and replaced with another stainless-steel disk.

Results

Synthesis and Characterization of Modified Silicas. As implied in the Introduction and shown experimentally in our earlier work,[25] fumed silicas functionalized with nonpolar groups are needed to form strong gels with polyethers. In particular, we found that R805, a commercial silica functionalized with

(31) Wood, N. F.; Chang, F. C. *J. Org. Chem.* **1965**, *30*, 2054.
(32) Matsuda, H.; Yamamoto, A.; Iwamoto, N.; Matsuda, S. *J. Org. Chem.* **1978**, *43*, 4567.
(33) Tolstikov, G. A.; Odinokov, V. N.; Galeeva, R. I.; Bakeeva, R. S.; Akhunova, V. R. *Chem. Nat. Compd. (Engl. Transl.)* **1982**, *18*, 219.
(34) Speier, J. L.; Webster, J. M.; Barnes, G. H. *J. Am. Chem. Soc.* **1957**, *79*, 974.

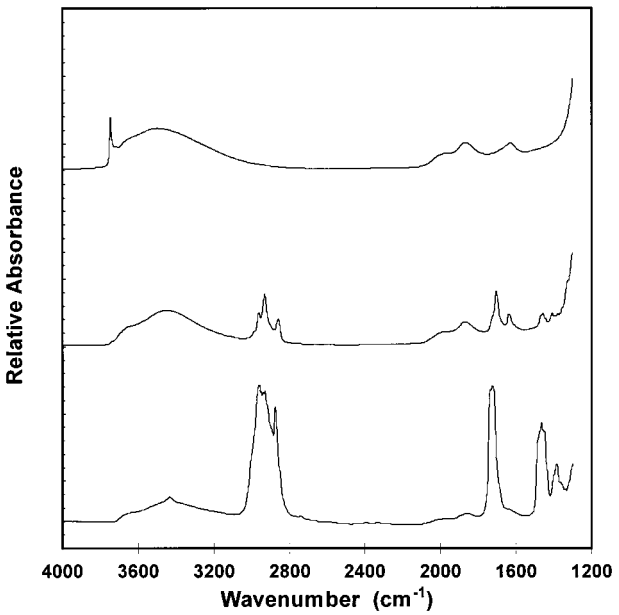

Figure 1. IR spectra of surface modified silicas. Top scan: Aerosil A-200 fumed silica; middle scan: A-200 modified with surface-bound methacrylates; bottom scan: cross-linked composite electrolyte after exhaustive extraction with acetone.

n-octyl groups, formed strong networks in PEGs and PEGDMEs. We examined a variety of fumed silica surface modifications, but based on the results obtained with R805, we initially focused on attaching polymerizable acrylates to fumed silica through C_8 tethers. As shown in Scheme 2, the synthesis of methacrylates suitable for tethering to silicas is straightforward, with the key steps being the introduction of the acrylate and trichlorosilane functionalities. During hydrosilylation to form **4a**, we found that the selectivity of the reaction was poor, and a large fraction of the acryloyl double bonds (**4a**, R = H) were hydrosilylated. Purification of the desired trichlorosilane product **4a** is difficult, so we switched to the methacrylate derivative (R = CH_3). The additional methyl group hinders hydrosilylation at the methacrylate double bond and cleanly yields the desired product. After hydrosilylation, volatile byproducts were removed under vacuum, and the methacrylate was used without further purification. Attachment of trichlorosilane **4b** to silica followed an established protocol. We also mimicked the C_8-tethered methacrylate by using a mixture of the commercially available octyltrimethoxysilane and trimethoxysilylpropyl methacrylate to modify silicas.

The functionalized silicas were characterized by IR and TGA measurements. As shown in Figure 1, (center trace) IR measurements show the expected C−H and C═O stretching bands for the tethered methacrylate. The IR spectra also show a broad band extending from 3000 to 3700 cm^{-1}. This band corresponds to residual hydroxyl groups that are inaccessible to surface-modifying reagents and to physisorbed water introduced during the preparation of the sample pellet. To estimate the degree of coverage (defined as the ratio of the moles of surface-attached groups to the moles of chemically accessible sites), we first titrated the silica with $LiAlH_4$ in diglyme. The number of chemically accessible hydroxyl groups measured by titration, 1.03 mmol/g, agreed with the value provided by the manufacturer.

Scheme 2. Preparation of Surface Modifiers for Fumed Silicas

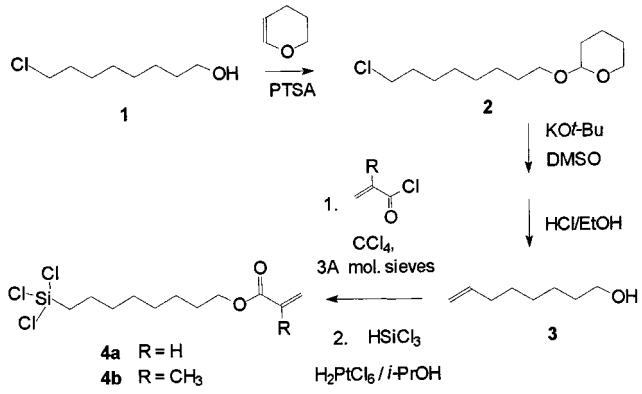

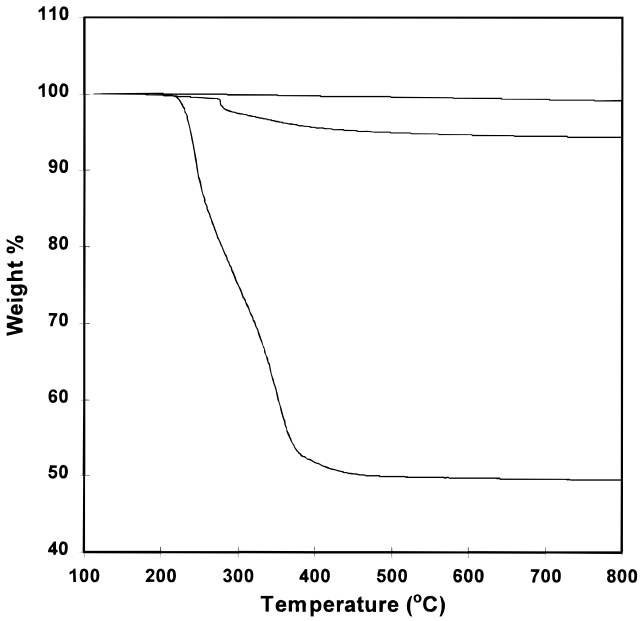

Figure 2. TGA scans of surface-modified fumed silicas. Top scan: Aerosil A-200 fumed silica; middle scan: A-200 modified with surface-bound methacrylates; bottom scan: cross-linked composite electrolyte after exhaustive extraction with acetone. Conditions: run in air at a heating rate of 10 °C/min.

Surface coverages were calculated by comparing the moles of unreacted trialkoxy or trichlorosilane recovered from the reaction with that expected based on the titration results. In most cases, we used an excess of the surface-modifying agent and obtained a maximum coverage of 50%. The exact value depended on the particular surface-modifying agent used. For silicas containing a mixture of modifiers (octyltrimethoxysilane plus trimethoxypropyl methacrylate, for example), the proportional coverage for the two surface modifiers was calculated from the mole ratio of the recovered unreacted alkoxysilanes. The TGA measurements also give a rough but independent measure of the surface coverage for the fumed silicas. As shown in Figure 2, the modified silica (center trace) loses about 6% of its weight at high temperatures in an oxidative atmosphere. If we assume that the measured weight loss corresponds to the loss of the hydrocarbon portion of the surface-modifying group, the 6% weight loss corresponds to about 50% coverage.

Preparation of Composite Electrolytes. Composite electrolytes were prepared by simply blending the

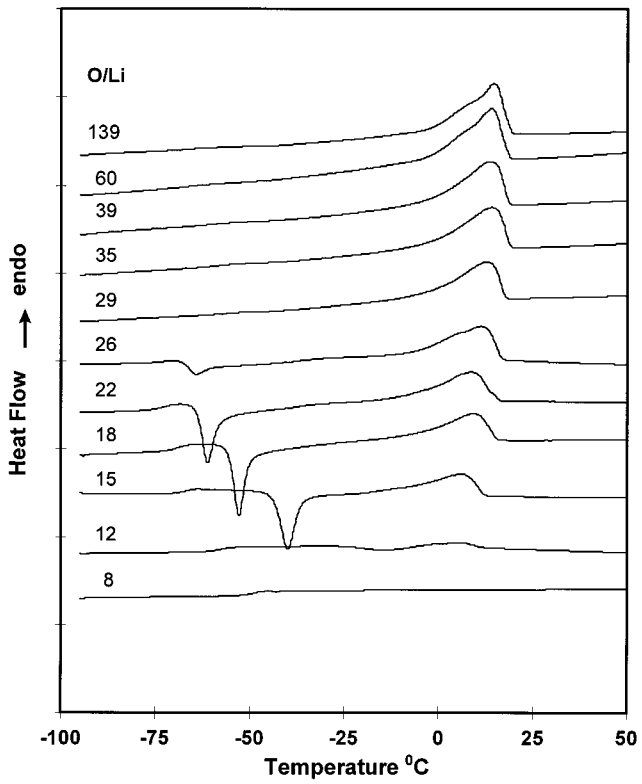

Figure 3. DSC second heating scans for PEGDME-500/$LiClO_4$ electrolytes. Conditions: run under He at a heating rate of 10 °C/min.

components of the electrolyte until homogeneous. The physical state of the composite depends on the type of modified fumed silica used as well as the amount of fumed silica and $LiClO_4$ in the composite. Those containing a low weight fraction of silica (<10%) or high O/Li ratios (>20) tend to be highly viscous liquids, whereas the use of higher weight fractions of silica or $LiClO_4$ led to the formation of rigid gels. This trend follows the increase in T_g seen for PEG electrolytes with increasing salt concentrations.

Our DSC measurements of PEGDME/$LiClO_4$ mixtures *without* added silica (Figure 3) illustrate some of these effects. These data are second scans, taken after flash quenching samples from 100 °C. At high O/Li ratios (low $LiClO_4$ content), DSC traces show a single broad melting peak that corresponds to the melting of a pure PEGDME phase. Addition of $LiClO_4$ causes both the melting point and the enthalpy for the transition to decrease and, at an O/Li ratio of 8, the transition is no longer detectable. A low temperature exothermic peak visible at intermediate salt concentrations corresponds to crystallization of a portion of the sample, presumably a pure PEGDME phase. A glass transition is also seen for these samples that, as expected, shifts to higher temperatures with increasing salt content. No crystallization was observed by DSC for samples with low salt contents because, for these materials, the PEGDME relaxation times are short and the PEGDME chains crystallize while being quenched from 100 °C.

DSC scans of composites *with silica* (Figure 4) are remarkable in that the thermal transitions for composites with and without silica appear at the same temperatures. These results show that the mobility of the PEGDME, as measured by T_g, is unaffected by the

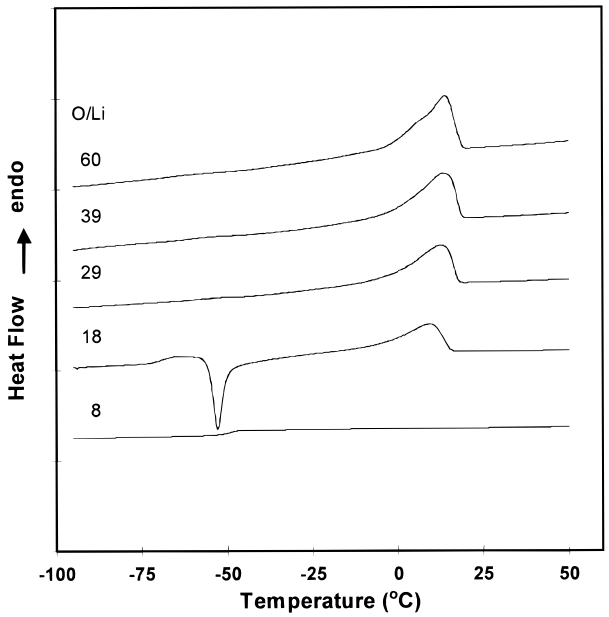

Figure 4. DSC second heating scans for PEGDME-500/fumed silica/$LiClO_4$ electrolytes. Conditions: run under He at a heating rate of 10 °C/min.

added silica. This result is strong experimental verification of the notion that the properties of the PEGDME phase are strongly decoupled from the added silica and that the improved mechanical properties provided by the fumed silica matrix are gained without significant losses in conductivity.

Cross-Linking Reactions. For cross-linking, AIBN and either methyl, butyl, or octyl methacrylate were included in the composite electrolytes. Of these three monomers, methyl methacrylate is somewhat volatile and tends to be lost from the composite during an evacuation step used to remove bubbles prior to curing. Thus, data reported here correspond to our experiments using butyl methacrylate. Cross-linking was carried out at room temperature with a medium-pressure Hg lamp. During irradiation, the characteristics of the composites evolved from being gel-like to those more typical of a cured silicone rubber. More detailed mechanical and rheological measurements are in progress and will be reported elsewhere. The cured composites are translucent and scatter light, with those cross-linked with methyl methacrylate the most clear and those prepared with octyl methacrylate the most cloudy. As discussed later, these results are in accord with increasing degrees of phase separation during cross-linking with decreasing polarity of the monomer used.

DSC traces for cross-linked composites containing $LiClO_4$ are shown in Figure 5. Qualitatively, these traces resemble those taken for composites before cross-linking. Some slight shifts in position and intensity are seen for the melting and crystallization transitions, but the values of the glass transitions are unchanged. Some hints of the chemistry that takes place during the cross-linking reaction can be inferred by monitoring changes in the IR spectrum of composites and the TGA data for cross-linked electrolytes. An electrolyte was prepared from PEGDME-500, surface-modified fumed silica, $LiClO_4$, and butyl methacrylate. As shown in Figure 1, the C═O and C═C vibrational bands characteristic of methacrylates are found in the spectrum of the un-

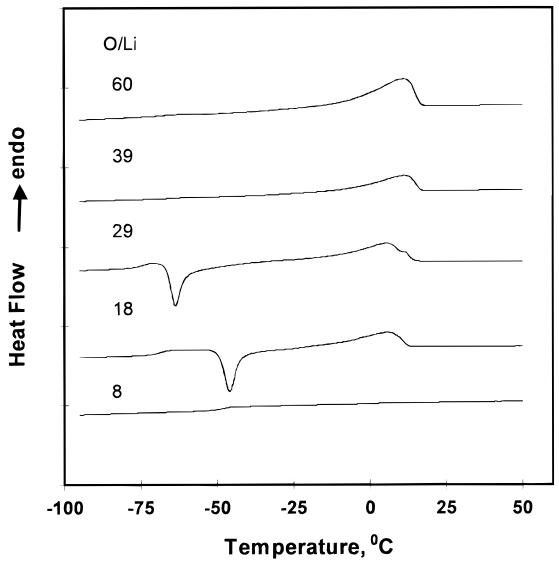

Figure 5. DSC second heating scans for cross-linked PEGDME-500/fumed silica/$LiClO_4$ electrolytes. Conditions: run under He at a heating rate of 10 °C/min.

cross-linked composite silica and, after irradiation, these bands shift to positions expected for a polymerized methacrylate. The bottom scan in Figure 1 corresponds to a cross-linked sample that was extracted exhaustively with acetone, a good solvent for poly(butyl methacrylate), and then dried. Prominent C═O and C−H stretching bands of the polymethacrylate dominate the spectrum. TGA scans of the same silica/polymer residue (Figure 2, bottom scan) show a 52% weight loss. The predicted weight loss, assuming all of the butyl methacrylate copolymerized with the methacrylates bound to the fumed silica, was 56%. Thus, we conclude that nearly all of the added monomer was chemically bound to the functionalized silica during cross-linking.

Freeze-fracture TEM imaging techniques were used to investigate changes in the structure and morphology of the silica composites upon curing. Replicas of electrolytes (Figure 6) before cross-linking show particulate features associated with the fumed silica network structure, but replicas made from cross-linked samples tend to be featureless. We interpret the difference between these two images to the changes in the nature of the silica network structure that occur during cross-linking. In un-cross-linked composites, poor adhesion between silica particles and between silica and the PEGDME-500 phase leads to fracture at the silica−PEGDME-500 interface. Polymerizing the added methacrylate binds the silica particles together and coats them with an amorphous polymer layer. Thus, fracture occurs within the mechanically weak PEGDME-500 phase, and the images of cross-linked samples appear smooth. Similar behavior has been observed in polymer latex films.[35]

Conductivity measurements show that the cross-linking reaction has little effect on the ionic conductivity of the composites. As shown in Figure 7, the room temperature data for a sample before and after cross-linking are nearly identical, $2-4 \times 10^{-4}$ S/cm. These results are consistent with the thermal analysis data that show little change in the T_g of composites after cross-linking. The conductivity depends on the lithium salt content and reaches a maximum at O/Li ratios of 20−40. The conductivity data were also analyzed with an Arrhenius plot (Figure 8), and from these plots, an interesting trend emerges. At high O/Li ratios, the slopes of the plots (activation energies) are similar, but as the O/Li ratio further decreases, the apparent activation energies steadily increase. In addition, the data taken at a given salt content are not linear and are suggestive of a phase transition near 55 °C. The nonlinearity is most pronounced for materials with high salt contents, which would be consistent with a crystalline−amorphous phase transition. However, to date we have been unable to verify such a transition by DSC or

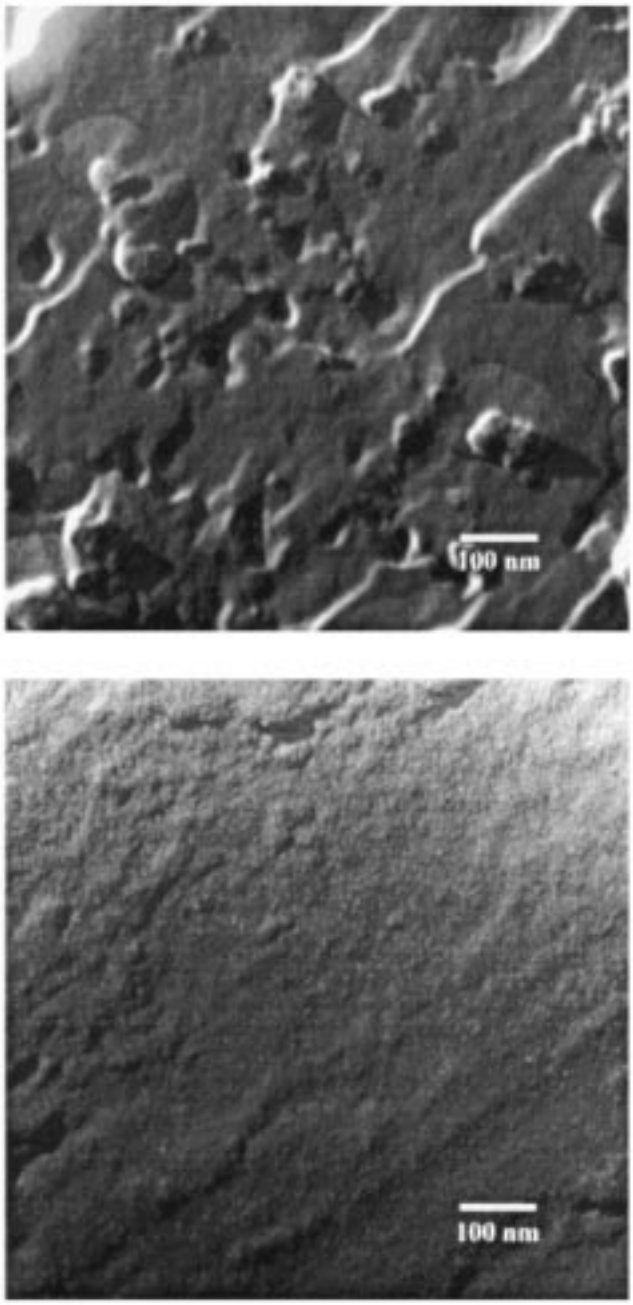

Figure 6. Freeze-fracture TEM replicas of composite electrolytes. Top: before cross-linking; bottom: after cross-linking.

(35) Steward, P. A.; Hearn, J.; Wilkinson, A. C.; Wilson, A. J.; Roulstone, B. J. *Permeation and Morphology in Polymer Latex Films Containing Leachable Additives*; Steward, P. A.; Hearn, J.; Wilkinson, A. C.; Wilson, A. J.; Roulstone, B. J., Eds., 1996; Vol. 648, pp 359−402.

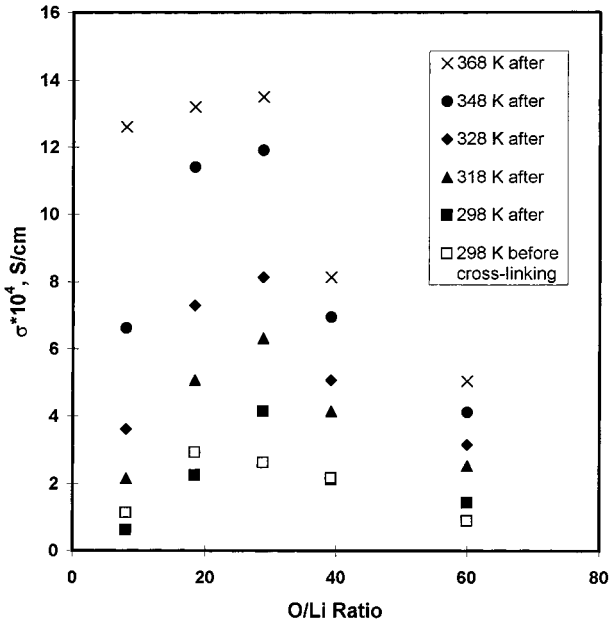

Figure 7. Conductivity of composite electrolytes at selected temperatures before and after cross-linking.

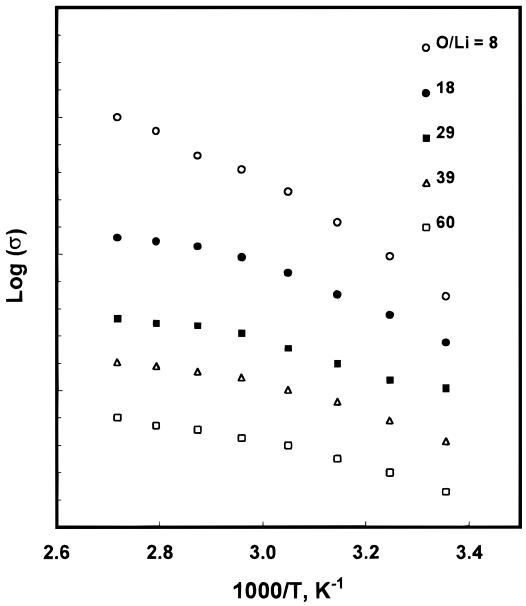

Figure 8. Arrhenius plots of the conductivity of cross-linked composite electrolytes. For clarity, the curves have been displaced vertically.

optical microscopy.

Discussion

The data presented in the Results Section show that highly processable, fumed silica-based electrolytes can be converted via photopolymerization into mechanically robust electrolytes with no apparent loss in conductivity. These results are in stark contrast to the data typically obtained with cross-linked polymer electrolytes. Usually cross-linking or the formation of interpenetrating network structures are accompanied by a large drop in conductivity, often by an order of magnitude.[36−38] The principal difference between the fumed silica system and traditional polymer electrolytes is that the mechanical properties of the composite and the ion-conducting characteristics are decoupled, and thus these two important characteristics can be optimized independently.

A simple model to understand these results can be based on simple phase-separation processes. For example, the addition of fumed silica to polyethers yields a two-phase system of the silica network structure that provides mechanical reinforcement of the composite and the polyether phase. Single-phase (or at least highly dispersed) polyether/silica mixtures can be prepared by appropriate surface modifications. For example, using standard chemical techniques, we attached short polyether chains to A-200. The modified silica completely dispersed in PEGDME-500 to give a clear low viscosity liquid. Similarly, there are many reports of the preparation of silicas by hydrolysis of tetraethoxysilane followed by surface modification to match the chemical characteristics of a particular matrix. These also form homogeneous solutions.[39,40] Mechanical properties appreciably better than those of the matrix itself require a silica network structure, which in turn requires a fumed silica that does not disperse, but instead aggregates. This structure must then be preserved in the cross-linked electrolyte.

Given that the starting point for our model is a two-phase system of silica dispersed in a polyether, the most important question is the fate of the monomer added to the composite before photopolymerization. We know from test polymerizations of methacrylates in PEGDME-500 that monomer/ether solutions are initially homogeneous, but become cloudy during polymerization, an obvious indication of phase separation. Moreover, polymerizations using octyl methacrylate yield the most turbid products, whereas the more polar methyl methacrylate appears to be the clearest. These results are in line with the relative differences in solubility parameters for the methacrylate polymers relative to PEGDME-500. Because none of these polymers are completely soluble in PEGDME-500, these results are not surprising but they do point to a model where polymer formation leads to phase separation. At least two limiting cases can be considered: the polymer (or oligomeric chains) phase separates and forms a distinct polymer phase as found in interpenetrating networks, or the polymer phase separates and segregates at the surface of the silica to form a phase consisting of surface-modified silica, monomer, and polymer. The first scenario is ruled out by extraction experiments carried out on cross-linked composites. Fully cross-linked samples were extracted with acetone, a good solvent for the methacrylate homopolymer, PEGDME-500, and lithium perchlorate, and the insoluble residue was analyzed. If pure homopolymer formed a distinct polymer phase, then it should be easily removed and the weight loss in the TGA experiment should be comparable to that seen for the surface-modified silica alone. The results,

(36) Nazri, G. A.; Meibuhr, S. G. *J. Electrochem. Soc.* **1989**, *136*, 2450.
(37) Wieczorek, W.; Such, K.; Florajanczyk, Z.; Stevens, J. R. *J. Phys. Chem.* **1994**, *98*, 6840−6850.
(38) Hudson, M. J.; Sequeira, C. A. C. *J. Electrochem. Soc.* **1995**, *142*, 4013.
(39) Sunkara, H. B.; Jethmalani, J. M.; Ford, W. T. *Chem. Mater.* **1994**, *6*, 362.
(40) Joseph, R.; Zhang, S.; Ford, W. T. *Macromolecules* **1996**, *29*, 1305.

however, point to nearly all of the monomer being chemically connected to the silica, and thus some version of the second scenario must be at play.

Additional evidence for strong segregation of the polymer and PEGDME-500 phases comes from comparisons of the mechanical properties of cross-linked electrolytes with those prepared without added monomer. Composites based on polymerizable fumed silica alone were mechanically weak and fractured easily, a sign of minimal chemical connectivity between adjacent silica particles. For strong composites, added monomer is needed to knit the silica particles into a mechanically stable framework. As noted in the Results Section, data sensitive to the segmental mobility of the PEGDME-500 phase, such as conductivity and T_g values, show little or no change with cross-linking.

Our model is also supported by literature reports, particularly those that describe the use of emulsion polymerization techniques to encapsulate inorganic particles and improve their dispersion in hydrophobic matrixes. A series of experiments[41−48] showed that surface modification of inorganic particles with anionic surfactants, titanates, or acrylates localized polymerization at the surface of the inorganic particles. Presumably, polymerization takes place in the hydrophobic chemical environment defined by the surface modifier. Some homopolymer also forms in the aqueous phase (the expected emulsion polymerization product), but by keeping the surfactant level below the critical micelle concentration, the amount of monomer dispersed in the aqueous phase and the amount of free polymer can be minimized. In a recent example of this approach, ethyl acrylate was polymerized by emulsion polymerization in the presence of silica that had been functionalized with acrylate groups.[49] The results reported are in accord with the added monomer separating from the continuous (aqueous) phase, copolymerizing with surface-bound acrylates, and encapsulating the silica particles. In our work, we believe the same phase separation process occurs, but instead of coating individual particles, we encapsulate the entire fumed silica network.

Based on our work and reports from the literature, phase separation of monomer from a continuous phase can be exploited to prepare surface-functionalized inorganic materials. These materials can be used to improve dispersion of the inorganic particles or, as in our case, to improve the mechanical properties of materials through formation of a network structure. We expect that by choosing appropriate fumed silica modifiers, this approach to the preparation of dimensionally stable composite materials can be generalized to both hydrophilic and hydrophobic polymer systems. Such experiments are currently in progress.

Acknowledgment. This work was funded by the Department of Energy, Basic Energy Sciences.

CM9704894

(41) Arai, M.; Arai, K.; Saito, S. *J. Polym. Sci., Polym. Chem. Ed.* **1982**, *20*, 1021−1029.
(42) Esther, A. W. G.; Herk, A. M. v.; German, A. L. *Polym. Prepr., ACS Div. Polym. Chem.* **1993**, *34*, 532−533.
(43) Hasegawa, M.; Arai, K.; Saito, S. *J. Polym. Sci., Part A: Polym. Chem.* **1987**, *25*, 3231−3239.
(44) Hasegawa, M.; Arai, K.; Saito, S. *J. Polym. Sci., Part A: Polym. Chem.* **1987**, *25*, 3117−3125.
(45) Hasegawa, M.; Arai, K.; Saito, S. *J. Appl. Polym. Sci.* **1987**, *33*, 411−418.
(46) Konno, M.; Shimizu, K.; Arai, K.; Saito, S. *J. Polym. Sci., Part A: Polym. Chem.* **1987**, *25*, 223−230.
(47) Hergeth, W.-D.; Starre, P.; Schmutzler, K.; Wartewig, S. *Polymer* **1986**, *29*, 1323−1326.
(48) Hergeth, W.-D.; Steinau, U.-J.; Bittrich, H.-J.; Simon, G.; Schmutzler, K. *Polymer* **1989**, *30*, 254−258.
(49) Bourgeat-Lami, E.; Espiard, P.; Guyot, A.; Gauthier, C.; David, L.; Vigier, G. *Die Angewandte Makromolekulare Chemie* **1996**, *242*, 105.